

Palladium Electrodeposition Onto a Carbon Fiber Ultramicroelectrode

Adrian S. Bravo-Rodriguez,¹ Giaan A. Álvarez-Romero,¹ Margarita Rivera,² Eduardo García-Sánchez,³
 Luis H. Mendoza-Huizar^{1,*}

¹ Universidad Autónoma del Estado de Hidalgo. Academic Area of Chemistry. Carretera Pachuca-Tulancingo Km. 4.5 Mineral de la Reforma México

² Instituto de Física, Universidad Nacional Autónoma de México, Ciudad de México, 04510, México

³ Universidad Autónoma de Zacatecas, Unidad Académica de Ingeniería Eléctrica, Av. Ramón López Velarde 801, Zacatecas, 98600, México

* Corresponding author's e-mail address: hhuizar@uaeh.edu.mx

RECEIVED: September 9, 2022 * REVISED: December 29, 2022 * ACCEPTED: January 3, 2023

Abstract: In the present work, it was conducted an electrochemical and kinetic study of Pd electrodeposition onto a 7 μm diameter CF (carbon fiber) ultramicroelectrode from an aqueous solution containing 1 mM of PdCl₂ and 1 M NH₄Cl as supporting electrolyte, at 25 °C and pH = 4.5. The voltammetric study suggests that at slow scan rates, radial diffusion is favored. The experimental current density transients obtained from the potentiostatic study were well predicted by an instantaneous nucleation and growth mathematical model, that considers the formation of separated hemispherical nuclei. The number of nuclei formed on the electrode surface is potential dependent, and increases as the applied potential diminishes.

Keywords: palladium, kinetics, electrodeposition, carbon fiber.

INTRODUCTION

PALLADIUM materials have found several applications in hydrogen storage,^[1,2] in the manufacture of anodes used in fuel cells,^[3–7] in redox reactions,^[8,9] and catalysis.^[9] However, due to the high price of these materials, much effort has been focused on reducing their cost by generating extended active areas with a small amount of this metal. This has been accomplished by electrodepositing palladium on carbonaceous substrates, which allows for the formation of a large electroactive area on an inexpensive substrate. In this sense, palladium has been electrodeposited on carbonaceous surfaces such as glassy carbon electrode (GCE),^[10–13] Highly Ordered Pyrolytic Graphite (HOPG),^[11,14–16] graphene,^[17] pencil graphite substrates,^[18,19] activated carbon felts,^[20] carbon fibers (CF),^[21,22] carbon nanotubes,^[23–28] and nanofibers^[23] electrodes. Specifically, palladium electrodeposited on carbon fiber electrodes has found applications as a flow-through anode for a microfluidic direct formate,^[7] direct formic acid^[4] and direct ethanol^[5,6] fuel cells. It has also been used as a non-enzymatic sensor capable of

quantifying peroxide,^[22] in the electro-oxidation of small organic molecules,^[4,29] and as potential materials for hydrogen storage applications.^[30]

Pd has been electrodeposited onto carbon fibers employing potentiodynamic,^[5–7] and potentiostatic^[4,22,30] methods. The preferred plating baths have been acid chloride plating baths. Pd was also electrodeposited from acid chloride ammoniacal solutions to keep the plating bath pH at 9.5 and ensure the formation of the Pd(NH₃)₄Cl₂ complex.^[28] They found that Pd is electrodeposited at potentials ranging from –0.2 to –0.8 V, and that the scan rate used for cyclic voltammetry electrodeposition influences not only the rate of Pd electrodeposition but also the microscopic morphology of Pd on the substrate.^[7] Pei et al carried out the electrodeposition of Pd onto CF by CV from a solution containing 2 mM K₂PdCl₄ at various pH values (pH 2.9, 5.0, 5.8, 7.0 and 8.0) in a potential range from –0.5 V to +0.9 V and they concluded that Pd electrodeposited at pH = 5.8 allowed the synthesis of a layer of Pd nanoparticles with an average size of about 10 nm.^[5] Sawangphruk et al., on the other hand, used cyclic voltammetry to cycle potential from 0 to –0.75 V vs.

Ag/AgCl in a plating bath containing 1 mM palladium(II) nitrate in 0.5 M H₂SO₄ at a scan rate of 0.01 V s⁻¹ for 10 cycles, yielding Pd nanorods with an average size of about 20 nm.^[6] However, to the best of our knowledge, there are no kinetic studies related to the palladium electrodeposition process from ammoniacal solutions onto carbon fiber ultramicroelectrodes. We consider that this kinetic information is necessary to understanding and controlling the formation of palladium clusters on these kinds of surfaces. Therefore, the purpose of the present study is to determine and analyze some kinetic parameters related to the Pd electrodeposition on CF electrodes.

EXPERIMENTAL SECTION

At 25 °C and pH = 4.5, Pd electrodeposits on CF were obtained from an aqueous solution containing 1 mM PdCl₂ and 1 M NH₄Cl as the supporting electrolyte. All solutions were prepared using analytical-grade reagents and ultrapure water (Millipore-Q system). The working electrode was a 7 μm-diameter carbon fiber that was manually separated with tweezers. After separation, the bunch was bound to a copper wire, approximately 5 cm long, using epoxy-silver conductive ink. This set was air-dried for 30 minutes before being placed into a glass capillary and the ends sealed with polyester resin. The ultramicroelectrodes were then exposed to an ethanolic solution before each experiment to eliminate the possibility of contaminants.^[31] A platinum wire was used as the counter electrode. All potentials are reported against an Ag/AgCl reference electrode. All electrochemical experiments were performed on a UNISCAN bipotentiostat connected to a personal computer running M370 software to allow experiment control and data acquisition. A potentiostatic study was carried out to analyze the nucleation and growth processes on the CF electrode. The behavior of the transients was analyzed by performing nonlinear adjustments using mathematical models reported in the literature. From these fits, kinetic parameters such as the diffusion coefficient and the number of nuclei were determined.

RESULTS AND DISCUSSION

Voltamperometric Study

Figure 1 shows cyclic voltammograms obtained from the CF/ 0.001 M PdCl₂ + 1 M NH₄Cl (solid line) and CF/ 1 M NH₄Cl (broken line) systems, at 25 °C and pH = 4.5 at a scan rate of 20 mV s⁻¹. A comparison between both voltammograms indicates that the changes in the current density are related to the Pd present in the plating bath. For the system containing Pd, note that the scanning potential

started at 0.80 V and proceeds towards the negative zone, at -0.07 V, the current density starts to diminish, and this potential value, E_{crist} , is related to the beginning of the Pd electrocrystallization process. At -0.23 V a cathodic peak A was recorded, the potential scan was inverted at -0.6 V and two cathodic peaks B and C were recorded at -0.2 V and 0.021 V, respectively. As the scan potential continued into the anodic zone, it is clear the formation of a crossover potential at null current at 0.18 V (E_{quia}), which may be associated with a conditional equilibrium potential.^[32] Also, observe the formation of an anodic peak D at -0.53 V, related to the oxidation of Pd electrodeposited at the direct scan. It is important to note here that the chemically dominant species under our experimental conditions is PdCl₄²⁻,^[17] and that the Pd reduction process is related to the following equation:



From Figure 1, it is possible to note that the potential reduction of the last reaction may be related to 0.18 V (E_{quia}). However, it has been reported that the reduction potential related to equation (1) is 0.28 V.^[17] It is worth noting here that different potential values for equation (1) have been reported in the literature and explained in terms of different degrees of palladium metal dispersed on the electrode surface.^[33]

In order to analyze the correspondence among peaks A, B, and C with peak D, it was recorded cyclic voltammograms at different inversion potentials at a constant scan rate of 20 mV s⁻¹, as shown in Figure 2. Note that when the inversion potential was -0.35 V, no anodic signal was recorded, but when the inversion potential was

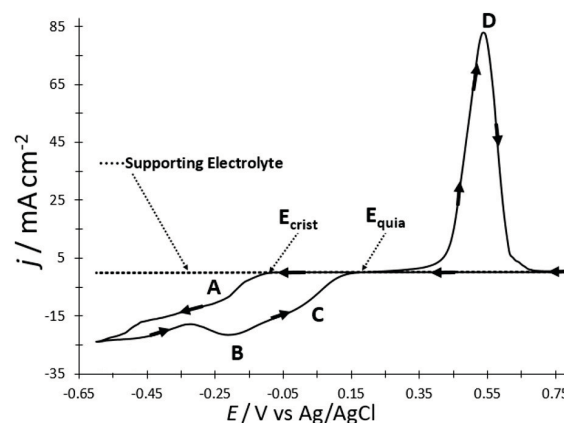


Figure 1. Typical cyclic voltammogram obtained in the CF/ 0.001 M PdCl₂ + 1 M NH₄Cl system at 25 °C and pH = 4.5. The potential scan was started at 0.8 V toward the negative direction with a scan potential rate of 20 mV s⁻¹. Arrows indicate the potential scan direction.

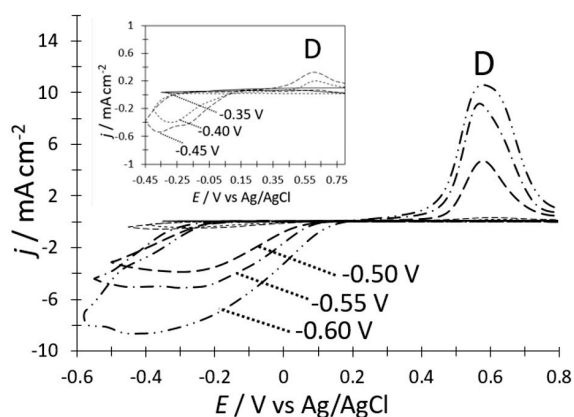


Figure 2. Cyclic voltammograms obtained in the CF / 0.001 M PdCl₂ + 1 M NH₄Cl system at 25 °C and pH = 4.5, and different inversion potentials indicated in the Figure. In all cases, the potential scan started at 0.800 V towards the negative direction with a potential scan rate of 20 mV s⁻¹.

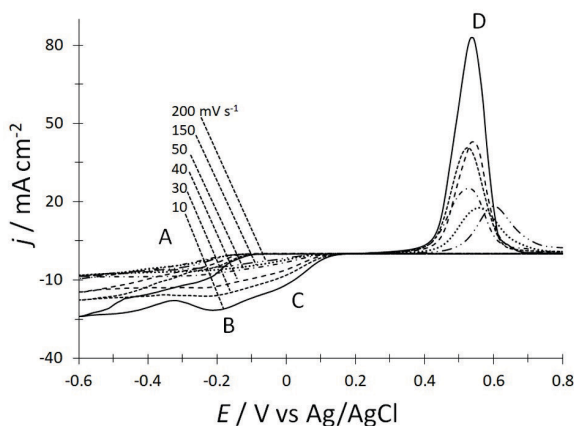


Figure 3. Cyclic voltammograms obtained in the CF / 0.001 M PdCl₂ + 1 M NH₄Cl system, at 25 °C and pH = 4.5, and different scan potential rates indicated in the figure. In all cases, the potential scan was started at 0.800 V towards the negative direction. Cathodic current density peaks (A, B, and C) and anodic peaks (D) are also indicated.

-0.45 V, the peak D appeared; at more negative inversion potential, this peak increased in function of inversion potential. These results suggest that the anodic peak D is related to peaks A, B, and C and corresponds to the Pd electrodeposited at the direct scan.

Potentiostatic Study

The kinetics and mechanism of Pd electrodeposition onto a carbon fiber electrode were measured by the potentiostatic technique. In all cases, the experiments involved the application of an initial potential (E_0) of 0.800 V on the CF surface. Under this potential condition, Pd deposition had not yet started, as could be easily noted from the previous

voltammetric study. After application of this initial potential, a second negative potential step (E_c) was applied onto the CF electrode surface for 10 s within the range of -0.23 – 0.58 V. Figure 4 shows the family of transients obtained at different applied potentials; note that at shorter times there is a falling current transient that, in the Pd electrodeposition case, may be associated with a double layer charge process.^[36] After this falling current, the j / t plot increases in each case without passing through a maximum. This behavior has been associated with a nucleation and growth process of separated hemispherical nuclei, which may be described for the instantaneous case by:^[37]

$$i(t) = \frac{zF\pi(2Dc)^{\frac{3}{2}}N_0M^{\frac{1}{2}}t^{\frac{1}{2}}}{\rho^{\frac{1}{2}}} \quad (2)$$

while in the progressive case by:^[37]

$$i(t) = \frac{4zFk_n\pi(Dc)^{\frac{3}{2}}N_0M^{\frac{1}{2}}t^{\frac{3}{2}}}{3\rho^{\frac{1}{2}}} \quad (3)$$

In these equations, F is the Faraday's constant (C mol⁻¹), D is the diffusion coefficient (cm² s⁻¹), c is the concentration (mol cm⁻³), z is the charge of ion, N_0 is the number of nuclei per unit area (cm⁻²), ρ is the metal density (g cm⁻³) and k_n is the rate constant for the nuclei formation.

According to equation (2), if one plots the current density associated with the nucleation process vs $t^{1/2}$, a linear behavior is obtained in the instantaneous case, while that for a progressive nucleation, the current density plotted vs $t^{3/2}$ is linear. The experimental current transients depicted in Figure 4 exhibited a linear behavior when the current density was plotted vs. $t^{1/2}$, see Figure 5, which indicates an instantaneous process with a nucleation and

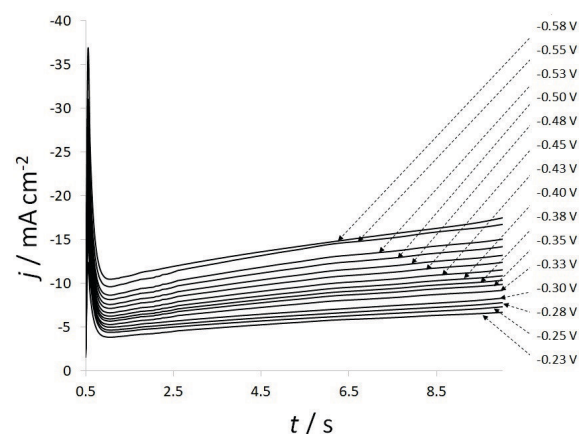


Figure 4. Set of experimental current transients recorded from the CF / 0.001 M PdCl₂ + 1 M NH₄Cl system, at 25 °C and pH = 4.5. In all cases, the starting potential of 0.800 V was applied to the CF electrode surface and $t = 10$ s.

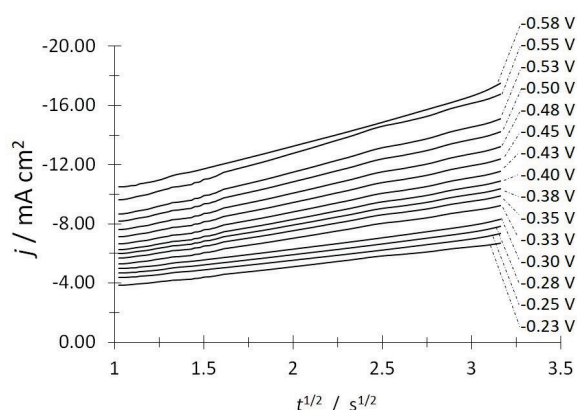


Figure 5. Plot of the experimental j vs $t^{1/2}$ according to equation (2). The experimental transients were recorded from the CF/ 0.001 M PdCl₂ + 1 M NH₄Cl system, at 25 °C and pH = 4.5.

growth process of separated hemispherical nuclei.^[38] No linear tendency was obtained when the current density was plotted vs. $t^{3/2}$ (not shown).

From the slope of the straight lines shown in Figure 5 and equation (2), it was possible to calculate the value of the diffusion coefficient and the number of nuclei formed at each applied potential at the electrode surface. The calculated average diffusion coefficient is $5.12 \times 10^{-5} \text{ cm}^2 \text{ s}^{-1}$. This value is greater than the $1.1 \times 10^{-6} \text{ cm}^2 \text{ s}^{-1}$ obtained by using the same electrolytic bath solution on a glassy carbon disc electrode of 0.0707 cm^2 .^[39] It should be noted that the diffusion coefficient evaluated in this study is nearly 46 times greater than that obtained on a conventional glassy carbon electrode.^[39] This is because near the surfaces of microdisk electrodes, radial diffusion becomes important. The latter causes the flux of the electroactive species towards the electrode surface to increase compared to conventional electrodes, where planar diffusion predominates. This results in an increase of the current density signal as the disk radius becomes smaller.^[40] Thus, the diffusion coefficient calculated in ultramicroelectrodes may be considered an apparent diffusion coefficient.^[41]

On the other hand, from the data reported in Table 1, observe that the number of nuclei is potential dependent, and they are increasing as the applied potential diminishes. Here, it is important to mention that in an instantaneous nucleation, the formation of nuclei on the electrode surface occurs in a single instant, they growth, and no more nuclei appear after this initial time. Then, the total current for the instantaneous case is given by the following equation:

$$i_r(t) = \sum_{i=1}^{N_0} i_i(t) = N_0 i_i(t) \quad (4)$$

where $i_r(t)$ is the total current in the time given, $i_i(t)$ is the current associated with each nucleus, which may be obtained as $i_i(t) = i_r(t)/N_0$ in each instant. Also, it is possible to evaluate the radius of the nucleus in each instant, considering the formation of a hemispherical nucleus and employing the well-known Faraday's electrolysis law as follows:

$$Q_i(t) = \int_{t_i}^{t_f} i_i(t) dt = \frac{\rho V_h z F}{M} = \frac{\rho \left(\frac{2}{3} \pi r_i^3\right) z F}{M} \quad (5)$$

$$r_i(t) = \left(\int_{t_i}^{t_f} i_i(t) dt \right)^{\frac{1}{3}} \left(\frac{3M}{2\pi z F \rho} \right)^{\frac{1}{3}} \quad (6)$$

In these equations $Q_i(t)$ is the electric charge related to the formation of a single nucleus in the range of time $[t_i - t_f]$, V_h and $r_i(t)$ are the volume and radius of a hemispheric nucleus, respectively. Figure 6 shows the plot of the variation of the radius nuclei, according to equation (6), in function of the time at each applied overpotential onto the CF electrode surface. In all cases, the integral into equation (6) was evaluated numerically, employing the experimental data reported in Figure 4. The calculation was started at $t_i = 1 \text{ s}$, where the nucleation process and the influence of the double layer have finished. In addition, for clarity, Figure 7a shows a graphical representation of how the Pd nucleus radius changes as a function of time and the specific case of a Pd nucleus obtained at -0.58 V is

Table 1. Number of nuclei formed from the system CF/ 0.001 M PdCl₂ + 1 M NH₄Cl system, at 25 °C and pH = 4.5, and different applied potentials, according to equation (2).

E / V	$N_0 \times 10^{-8} / \text{cm}^{-2}$
-0.58	1.523
-0.55	1.542
-0.53	1.534
-0.5	1.497
-0.48	1.496
-0.45	1.434
-0.43	1.397
-0.40	1.378
-0.38	1.361
-0.35	1.343
-0.33	1.343
-0.30	1.224
-0.28	1.204
-0.25	1.219
-0.23	1.189

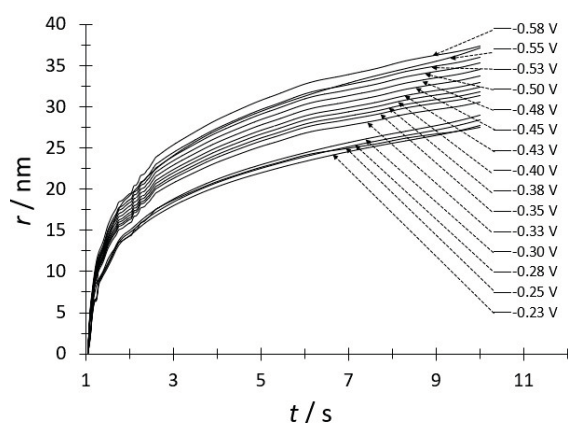


Figure 6. Variation of the nucleus radius as a function of time, obtained using equation (6) and experimental data from the system CF / 0.001 M PdCl₂ + 1 M NH₄Cl system, at 25 °C and pH = 4.5, and at various applied potentials onto the CF electrode.

analyzed. Note that the nucleus radius increases rapidly in the first 3 seconds and then decreases, most likely due to increased competition for metal ions by the growing nuclei and a significant amount of material needed to increase the radius of the hemisphere as time increases, see Figure 7b.

Also, with the data reported in Table 1, it is possible to predict the distribution of the nuclei formed on the carbon fiber substrate, considering that equation (2) was derived using a random distribution law of nuclei points.^[42]

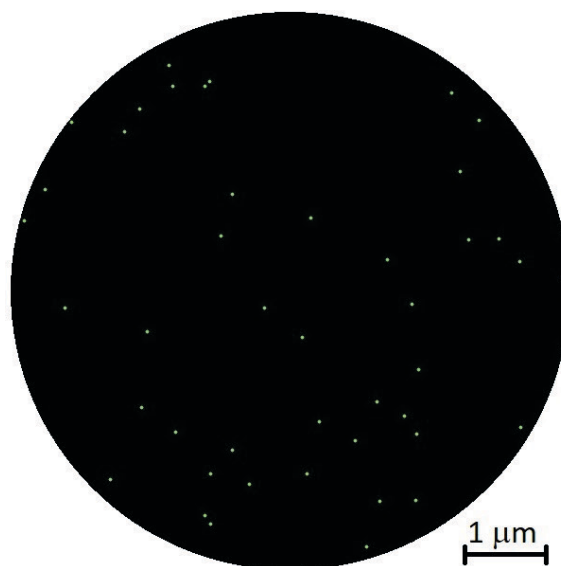


Figure 8. Graphical representation for random distribution of nuclei obtained at -0.58 V onto a CF electrode, considering the data reported in Table 1.

Figure 8 shows a simulation considering the formation of separated hemispherical nuclei and a random distribution of nuclei onto a disc electrode of 7 μm² in diameter when a -0.58 V potential is applied onto the carbon fiber electrode. At this potential value, there are formed 59 nuclei in an area of 39 μm². This image was generated through the

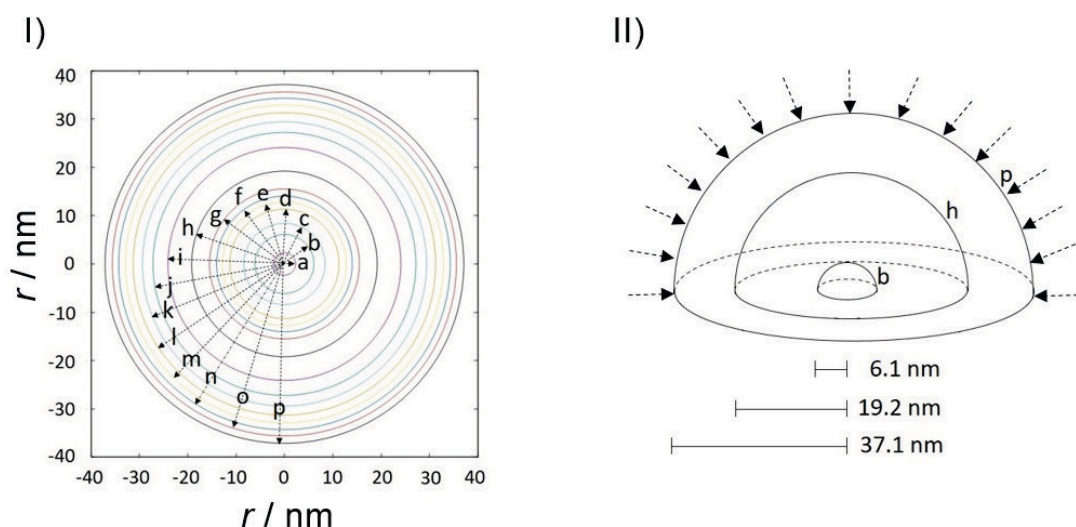


Figure 7. I) Graphical representation of an Pd hemispherical nucleus radius, obtained by using equation (6) and experimental data from the system CF/0.001 M PdCl₂ + 1 M NH₄Cl system, at 25 °C the pH = 4.5, at -0.58 V, I) at different times a=1.1 s, b = 1.15 s, c = 1.2 s, d = 1.3 s, e = 1.4 s, f = 1.5 s, g = 1.6 s, h = 2 s, i = 3 s, j = 4 s, k = 5 s, l = 6 s, m = 7 s, n = 8 s, o = 9 s, and p = 10 s. and II) A depiction of the radial diffusion in the growth of a Pd hemispherical nucleus.

Gnuplot software,^[43] its comparison with microscopic and morphological studies is beyond the scope of this work and it will be carried out at next works to evaluate the ability of the nucleation model employed to predict the distribution of the Pd nuclei onto the CF electrode surface at different times and with different applied overpotentials.

CONCLUSIONS

An electrochemical study about the Pd electrodeposition onto a CF of 7 μm of critical diameter from an aqueous solution containing PdCl_2 at 0.001 M with 1 M NH_4Cl as the supporting electrolyte, was conducted at overpotential conditions through voltamperometric and potentiostatic studies. The analysis of the electric charge involved and the number of nuclei formed in function of time allows us to predict the evolution of the nucleus radius in function of time. Also, the value of the diffusion coefficient obtained on the CF electrode, which is $5.12 \times 10^{-5} \text{ cm}^2 \text{ s}^{-1}$, may be considered an apparent diffusion coefficient because its value is increased in comparison to that obtained with conventional electrodes due to the influence of radial diffusion.

Acknowledgment. ASBR acknowledges CONACYT for the scholarship granted for Doctoral studies. Authors gratefully acknowledge financial support from CONACYT (project CB2015-257823) and to the Universidad Autónoma del Estado de Hidalgo. Also, the authors thankfully acknowledge the computer resources, technical expertise and support provided by the Laboratorio Nacional de Supercómputo del Sureste de México, CONACYT member of the network of national laboratories through the project No. 202203072N. LHMH acknowledges to the SNI for the distinction of his membership and the stipend received.

REFERENCES

- [1] J. O. Besenhard, U. Krebber, *J. Electrochem. Soc.* **1989**, 136, 3608–3610.
<https://doi.org/10.1149/1.2096518>
- [2] N. Semagina, A. Renken, L. Kiwi-Minsker, *Chem. Eng. Sci.* **2007**, 62, 5344–5348.
<https://doi.org/10.1016/j.ces.2006.11.023>
- [3] C. Bianchini, P. K. Shen, *Chem. Rev.* **2009**, 109, 4183–4206.
https://doi.org/10.1021/CR9000995/ASSET/CR9000995.FP.PNG_V03
- [4] K. K. Maniam, V. Muthukumar, R. Chetty, *Int. J. Hydrogen Energy*, **2016**, 41, 18602–18609.
<https://doi.org/10.1016/j.ijhydene.2016.08.064>
- [5] H. Y. Pei, C. H. Lin, W. Lin, C. J. Yuan, *Catalysts* **2021**, 11, 1–13. <https://doi.org/10.3390/catal11020248>
- [6] M. Sawangphruk, A. Krittayavathananon, N. Chinwipas, *J. Mater. Chem. A* **2012**, 1, 1030–1034.
<https://doi.org/10.1039/C2TA00659F>
- [7] T. Zhang, X. Zhu, D. D. Ye, R. Chen, Y. Zhou, Q. Liao, *Nanoscale* **2020**, 12, 20270–20278.
<https://doi.org/10.1039/d0nr05134a>
- [8] S. A. Miscoria, G. D. Barrera, G. A. Rivas, *Electroanalysis* **2002**, 14, 981–987.
<https://doi.org/10.1002/1521-4109>
- [9] M. Rajkumar, C. Pon Hong, S.-M. Chen, *Int. J. Electrochem. Sci.* **2013**, 8, 5262–5274.
<http://www.electrochemsci.org/papers/vol8/80405262.pdf>
- [10] T. Alemu, B. D. Assresahegn, T. R. Soreta, *Port. Electrochim. Acta* **2014**, 32, 21–33.
<https://doi.org/10.4152/pea.201401021>
- [11] O. Corduneanu, V. C. Diculescu, A. M. Chiorcea-Paquim, A. M. Oliveira-Brett, *J. Electroanal. Chem.* **2008**, 624, 97–108.
<https://doi.org/10.1016/j.jelechem.2008.07.034>
- [12] I. E. Espino-López, M. Romero-Romo, M. G. M. de Oca-Yemha, P. Morales-Gil, M. T. Ramírez-Silva, J. Mostany, M. Palomar-Pardavé, *J. Electrochem. Soc.* **2019**, 166, D3205–D3211.
<https://doi.org/10.1149/2.0251901JES/XML>
- [13] Z. Li, J. Zhang, Y. Zhou, S. Shuang, C. Dong, M. M. F. Choi, *Electrochim. Acta* **2012**, 76, 288–291.
<https://doi.org/10.1016/j.electacta.2012.05.020>
- [14] M. Alpuche-Aviles, F. Farina, G. Ercolano, P. Subedi, S. Cavaliere, D. Jones, J. Rozière, M. A. Alpuche-Aviles, F. Farina, G. Ercolano, P. Subedi, S. Cavaliere, D. J. Jones, J. Rozière, *Nanomater.* **2018**, 8, 668.
<https://doi.org/10.3390/NANO8090668>
- [15] V. C. Diculescu, A. M. Chiorcea-Paquim, O. Corduneanu, A. M. Oliveira-Brett, *J. Solid State Electrochem.* **2007**, 11, 887–898.
<https://doi.org/10.1007/s10008-007-0275-7>
- [16] L. H. Mendoza-Huizar, D. Garrido-Márquez, C. H. Rios-Reyes, M. Rivera, E. García-Sánchez, C. Galán-Vidal, *J. Clust. Sci.* **2015**, 26, 337–346.
<https://doi.org/10.1007/s10876-014-0837-7>
- [17] M. Rezaei, S. H. Tabaian, D. F. Haghshenas, *Electrochim. Acta* **2013**, 87, 381–387.
<https://doi.org/10.1016/j.electacta.2012.09.092>
- [18] M. Rezaei, S. H. Tabaian, D. F. Haghshenas, *Electrochim. Acta* **2011**, 59, 360–366.
<https://doi.org/10.1016/j.electacta.2011.10.081>
- [19] M. A. Aziz, A. N. Kawde *Microchim. Acta* **2013**, 180, 837–843.
<https://doi.org/10.1007/s00604-013-1000-0>
- [20] M. L. Bosko, F. A. Marchesini, L. M. Cornaglia, E. E. Miró, *Catal. Commun.* **2011**, 16, 189–193.
<https://doi.org/10.1016/j.catcom.2011.09.034>

- [21] A. D. Jannakoudakis, *Synth. Met.* **1991**, 39, 303–309. [https://doi.org/10.1016/0379-6779\(91\)91756-Z](https://doi.org/10.1016/0379-6779(91)91756-Z)
- [22] A. McConville, A. Mathur, J. Davis, *IEEE Sens. J.* **2019**, 19, 34–38. <https://doi.org/10.1109/JSEN.2018.2872895>
- [23] J. C. Bradley, S. Babu, P. Ndungu, *Fullerenes Nanotub. Carbon Nanostructures* **2005**, 13, 227–237. <https://doi.org/10.1081/FST-200056245>
- [24] D. Gioia, I. G. Casella, *Sensors Actuators, B Chem.* **2016**, 237, 400–407. <https://doi.org/10.1016/j.snb.2016.06.109>
- [25] C. Te Hsieh, Y. Y. Liu, Y. S. Cheng, W. Y. Chen, *Electrochim. Acta* **2011**, 56, 6336–6344. <https://doi.org/10.1016/j.electacta.2011.05.025>
- [26] C. H. Lee, S. C. Wang, C. J. Yuan, M. F. Wen, K. S. Chang, *Biosens. Bioelectron.* **2007**, 22, 877–884. <https://doi.org/10.1016/j.bios.2006.03.008>
- [27] S. H. Lim, J. Wei, J. Lin, Q. Li, J. KuaYou, *Biosens. Bioelectron.* **2005**, 20, 2341–2346. <https://doi.org/10.1016/j.bios.2004.08.005>
- [28] S. Mubeen, T. Zhang, B. Yoo, M. A. Deshusses, N. V. Myung, *J. Phys. Chem. C* **2007**, 111, 6321–6327. <https://doi.org/10.1021/jp067716m>
- [29] A. T. Mathew, K. B. Akshaya, T. P. Vinod, A. Varghese, L. George, *ChemistrySelect* **2020**, 5, 3283–3294. <https://doi.org/10.1002/slct.201904432>
- [30] S. H. Hwang, Y. K. Kim, H. J. Seo, S. M. Jeong, J. Kim, S. K. Lim, *Nanomaterials* **2021**, 11, 1–13. <https://doi.org/10.3390/NANO11071830/S1>
- [31] A. Gevaerd, B. M. Da Silva, P. R. De Oliveira, L. H. Marcolino Júnior, M. F. Bergamini, *Anal. Methods* **2020**, 12, 3608–3616. <https://doi.org/10.1039/D0AY01050B>
- [32] A. Rojas-Hernández, M. T. Ramírez, J. G. Ibáñez, I. González, *J. Electrochem. Soc.* **1991**, 138, 365–371. <https://doi.org/10.1149/1.2085590>
- [33] O. V. Belousov, Y. V. Saltykov, L. I. Dorokhova, L. A. Solov'ev, S. M. Zharkov, *Russ. J. Phys. Chem. A* **2008**, 82, 647–650. <https://doi.org/10.1134/s0036024408040249>
- [34] S. Ching, R. Dudek, E. Tabet, *J. Chem. Educ.* **1994**, 71, 602–605. <https://doi.org/10.1021/ed071p602>
- [35] M. J. Peña, R. Celdran, R. Duo, *J. Electroanal. Chem.* **1994**, 367, 85–92. [https://doi.org/10.1016/0022-0728\(93\)03028-N](https://doi.org/10.1016/0022-0728(93)03028-N)
- [36] M. H. Hölzle, U. Retter, D. M. Kolb, *J. Electroanal. Chem.* **1994**, 371, 101–109. [https://doi.org/10.1016/0022-0728\(93\)03235-H](https://doi.org/10.1016/0022-0728(93)03235-H)
- [37] G. J. Hills, D. J. Schiffrin, J. Thompson, *Electrochim. Acta* **1974**, 19, 657–670. [https://doi.org/10.1016/0013-4686\(74\)80008-3](https://doi.org/10.1016/0013-4686(74)80008-3)
- [38] G. Hills, A. Kaveh Pour, B. Scharifker, *Electrochim. Acta* **1983**, 28, 891–898. [https://doi.org/10.1016/0013-4686\(83\)85164-0](https://doi.org/10.1016/0013-4686(83)85164-0)
- [39] A. S. Bravo-Rodriguez, L. H. Mendoza-Huizar, *ECS Trans.* **2017**, 76(1), 29–35. <https://doi.org/10.1149/07601.0029ecst>
- [40] T. M. Braun, D. Josell, T. P. Moffat, *J. Electrochem. Soc.* **2020**, 167, 082509. <https://doi.org/10.1149/1945-7111/AB8E86>
- [41] J. A. Corona-Castro, G. A. Álvarez-Romero, M. Rivera, J. M. Sausedo-Solorio, C. H. Rios-Reyes, L. H. Mendoza-Huizar, *Croat. Chem. Acta* **2021**, 93, 237–243. <https://doi.org/10.5562/CCA3771>
- [42] G. Luo, Y. Yuan, D. Y. Li, N. Li, G. H. Yuan, *Coatings* **2022**, 12(8) 1195. <https://doi.org/10.3390/coatings12081195>
- [43] T. Williams, C. Kelley, C. Bersch, H.-B. Bröker, J. Campbell, R. Cunningham, D. Denholm, G. Elber, R. Fearick, C. Grammes, L. Hart, L. Hecking, P. Juhász, T. Koenig, D. Kotz, et al., **1986**. <http://sourceforge.net/projects/gnuplot>
 Accessed December 19, 2022.